NMR approaches for monitoring domain orientations in calcium-binding proteins in solution using partial replacement of Ca^{2+} by Tb^{3+}

Rodolfo R. Biekofsky[a], Frederick W. Muskett[b], Jürgen M. Schmidt[a], Stephen R. Martin[c], J. Peter Browne[c], Peter M. Bayley[c], James Feeney[a,*]

[a] *Molecular Structure Division, National Institute for Medical Research, The Ridgeway, Mill Hill, London NW7 1AA, UK*
[b] *MRC Biomedical NMR Centre, National Institute for Medical Research, The Ridgeway, Mill Hill, London NW7 1AA, UK*
[c] *Physical Biochemistry Division, National Institute for Medical Research, The Ridgeway, Mill Hill, London NW7 1AA, UK*

Received 9 September 1999; received in revised form 7 October 1999

Abstract **This work shows that the partial replacement of diamagnetic Ca^{2+} by paramagnetic Tb^{3+} in Ca^{2+}/calmodulin systems in solution allows the measurement of interdomain NMR pseudocontact shifts and leads to magnetic alignment of the molecule such that significant residual dipolar couplings can be measured. Both these parameters can be used to provide structural information. Species in which Tb^{3+} ions are bound to only one domain of calmodulin (the N-domain) and Ca^{2+} ions to the other (the C-domain) provide convenient systems for measuring these parameters. The nuclei in the C-domain experience the local magnetic field induced by the paramagnetic Tb^{3+} ions bound to the other domain at distances of over 40 Å from the Tb^{3+} ion, shifting the resonances for these nuclei. In addition, the Tb^{3+} ions bound to the N-domain of calmodulin greatly enhance the magnetic susceptibility anisotropy of the molecule so that a certain degree of alignment is produced due to interaction with the external magnetic field. In this way, dipolar couplings between nuclear spins are not averaged to zero due to solution molecular tumbling and yield dipolar coupling contributions to, for example, the one-bond ^{15}N-^{1}H splittings of up to 17 Hz in magnitude. The degree of alignment of the C-domain will also depend on the degree of orientational freedom of this domain with respect to the N-domain containing the Tb^{3+} ions. Pseudocontact shifts for NH groups and ^{1}H-^{15}N residual dipolar couplings for the directly bonded atoms have been measured for calmodulin itself, where the domains have orientational freedom, and for the complex of calmodulin with a target peptide from skeletal muscle myosin light chain kinase, where the domains have fixed orientations with respect to each other. The simultaneous measurements of these parameters for systems with domains in fixed orientations show great potential for the determination of the relative orientation of the domains.**

© 1999 Federation of European Biochemical Societies.

Key words: Calcium binding protein; Calmodulin; Terbium binding; Paramagnetic lanthanide ion; Pseudocontact shift; Residual dipolar coupling

1. Introduction

For many multidomain proteins in solution little information is available to accurately position the domains with respect to each other. For example, in NMR structure determinations, interdomain nuclear Overhauser enhancement (NOE) crosspeaks are frequently unobserved for multidomain proteins [1]. Recent studies of proteins partially aligned in solution have shown the usefulness of measuring anisotropic spin interactions, such as residual dipolar couplings, for obtaining unique long-range structural information [2,3]. Fischer and coworkers have recently applied this approach to study the domain orientation and dynamics of a two-domain fragment from the protein barley lectin in different liquid crystal solutions [4].

The present communication examines the potential of using paramagnetic lanthanide ions (Ln^{3+}) as an NMR approach for monitoring interdomain phenomena in multidomain calcium-binding proteins, such as calmodulin or troponin C. Lanthanide ions have been frequently used as paramagnetic probes for the Ca^{2+} ion in NMR studies [5,6]. However, most of the structural NMR work involving paramagnetic ions and calcium-binding proteins has been done on single-domain proteins or single-domain fragments of multidomain proteins. Lee and Sykes have used the substitution of the paramagnetic lanthanide Yb^{3+} ion for the calcium ions bound to the CD and EF sites of carp parvalbumin to study the structure of this single-domain protein in solution [5]. Recently, the solution structure of the $(Ce^{3+})_2$ complex of the N-domain of calmodulin has been solved employing paramagnetic T_1 relaxation enhancements and pseudocontact shifts introduced by the Ce^{3+} ions, to supplement conventional NOE-based distance constraints [6].

In the present work the binding characteristics and magnetic properties of Tb^{3+} as a candidate for producing long-range pseudocontact shifts (PCSs) and residual dipolar couplings (RDCs) in calmodulin systems in solution are investigated. Calmodulin is a 148-residue calcium-binding protein that can bind up to four Ca^{2+} ions and is organised into two structurally similar globular domains, usually referred to as the N-domain (residues 1–78) and the C-domain (residues 81–148), connected by a flexible linker [7]. Each domain contains a pair of EF-hands or helix-loop-helix motifs and can therefore bind two Ca^{2+} ions [8]. The Ca^{2+} ions bind with higher affinity to the C-domain than to the N-domain, and the NMR changes observed throughout a Ca^{2+} titration at 11.7 T (^{1}H frequency of 500 MHz) occur in slow exchange for the C-domain, yielding separate signals for the different species in solution, and in fast exchange for the N-domain, leading to signals with average chemical shifts for nuclei exchanging between bound and unbound species [9]. Provided that the structure of each domain is known from either NOE-

*Corresponding author. Fax: (44) (208) 906-4477.
E-mail: jfeeney@nimr.mrc.ac.uk

Abbreviations: CaM, calmodulin; DSS, sodium 2,2-dimethyl-2-silapentane-5-sulphonate; IPAP, in phase-anti phase; HSQC, heteronuclear single quantum coherence spectroscopy; Ln^{3+}, trivalent lanthanide ion; NOE, nuclear Overhauser enhancement; PCS, pseudocontact shift; RDC, residual dipolar coupling; skMLCK, skeletal muscle myosin light chain kinase

0014-5793/99/$20.00 © 1999 Federation of European Biochemical Societies. All rights reserved.
PII: S0014-5793(99)01410-6

based NMR methods or from X-ray crystallography, the novel combined use of long-range constraints from pseudocontact shifts and residual dipolar couplings in Tb^{3+}-bound calmodulin complexes has considerable potential for the determination of the relative orientation of the domains with respect to each other in solution.

2. Materials and methods

2.1. Protein

The cDNA encoding *Drosophila melanogaster* calmodulin, kindly supplied by K. Beckingham in the pOTSNco12 vector [10], was transformed into the *Escherichia coli* cell line AR58 [11] and used for the expression of the ^{15}N-labelled calmodulin. After the bacterial cell culture was grown, the calmodulin (CaM) was isolated and purified to homogeneity as described elsewhere [9].

The purified calmodulin was concentrated to 2.2 mM (25 mM Tris-HCl pH 7.5, 500 mM KCl, 10 mM $CaCl_2$ and 5 mM EDTA). The apo-protein was prepared by treating with a further 10 mM EDTA and passing through a Pharmacia PD10, Sephadex G25 desalting column equilibrated and eluted with 111 mM KCl (pre-treated with Chelex (Sigma)). After the pH of the eluted protein was adjusted to pH 6.5, the concentration was determined spectrophotometrically using $\varepsilon_{259\,nm} = 2179\ M^{-1}\ cm^{-1}$ [10] and D_2O was added to give 90% H_2O:10% D_2O. The $(Ca^{2+})_4$-calmodulin was prepared by adding 4 equivalents of $CaCl_2$ (a $[Ca^{2+}]$/[CaM] ratio of 4) plus 100 μM excess of $CaCl_2$ to the apo-protein eluting from the PD10 column.

2.2. Peptide

The peptide **KRRWKKNFIAVSAANRFK** (WFF peptide), residues 1–18 of the M13 calmodulin target sequence of skeletal muscle myosin light chain kinase (skMLCK) was synthesised on an Applied Biosystems 430A peptide synthesiser and purified by HPLC on a C18 column. Purity and molecular weight were further checked using a VG Platform electrospray mass spectrometer. The WFF peptide had free carboxy- and amino-termini. The concentration of the WFF peptide was determined spectrophotometrically using $\varepsilon_{280\,nm} = 5690\ M^{-1}\ cm^{-1}$ [12].

2.3. Complex

The calmodulin-WFF complex was prepared by adding 1 equivalent of WFF to the $(Ca^{2+})_4$-calmodulin complex (a [WFF]/[CaM] ratio of 1). The pH was adjusted to 6.5 and the sample made up to give 90% H_2O/10% D_2O with a final concentration of 1.4 mM in 100 mM KCl.

2.4. Titration

A stock solution of 50 mM $TbCl_3$ in 90% H_2O/10% D_2O was prepared from a standard 1 M $TbCl_3$ solution. For each titration point an aliquot of 0.4 μl (a $[Ca^{2+}]$/[CaM] ratio of 0.33) of this stock $TbCl_3$ solution was added to the protein solution and mixed thoroughly. The changes in pH caused by $TbCl_3$ additions were negligible. Similar procedures were followed for the preparation of a stock solution of 50 mM $CaCl_2$ in 90% H_2O/10% D_2O for the protein titration with Ca^{2+} ions.

2.5. NMR spectroscopy

All NMR experiments were performed on Varian Unity or Unity Plus spectrometers operating at ^1H Larmor frequencies of 600 or 500 MHz respectively. All data were collected in phase-sensitive mode using the method of States and coworkers [13]. Spectra from the Tb^{3+} and Ca^{2+} titrations of the protein were acquired at 25°C. Spectra used for the measurement of PCS and RDC values were acquired at 35°C.

^1H-^{15}N heteronuclear single quantum coherence (HSQC) spectra [14,15] were acquired at 500 MHz with 1184 complex points in t_2 (148 ms acquisition time) with a spectral width of 8000 Hz and the ^1H carrier set to the water frequency; 128 complex points were collected in t_1 (51 ms acquisition time) with a spectral width of 2500 Hz and the ^{15}N carrier at 119.1 ppm. Residual dipolar couplings were extracted from 2D in phase-anti phase (IPAP) ^1H-^{15}N HSQC spectra [16] at 600 MHz. Spectra were acquired with 1184 complex points in t_2 (148 ms acquisition time) with a spectral width of 8000 Hz, and 270 complex points were collected in t_1 (108 ms acquisition time) with spectral widths of 3000 Hz.

All spectra were processed using the Felix software package (Felix, version 2.3, 1993, Biosym Technologies, Inc., San Diego, CA, USA). For each spectrum a 90° shifted sine-bell squared apodisation function was applied, and the data were zero-filled once in each dimension prior to Fourier transformation. Spectra were analysed using the program XEASY [17]. ^1H-^{15}N one-bond splittings in the F1 dimension of the IPAP spectra were measured in Hz using an adaptation of the trace-alignment concept [18]. The 2BBM solution structure [19] was examined using INSIGHT II Version 97.0 Molecular Modelling Simulation (Molecular Simulations, Inc., San Diego, CA, USA).

^1H chemical shifts were referenced to sodium 2,2-dimethyl-2-silapentane-5-sulphonate (DSS) and ^{15}N chemical shifts referenced to liquid NH_3 [20]. The previously assigned ^1H and ^{15}N resonances of apo- and holo-calmodulin and its complex with the target peptide from skMLCK ([11,21,22]; M. Ikura, personal communication) were used to identify signals from nuclei of the $(Ca^{2+})_4$-calmodulin species in each system.

3. Results

3.1. Tb^{3+} titration of $(Ca^{2+})_4$-calmodulin

A Tb^{3+} titration using 2D ^1H-^{15}N HSQC NMR spectra of ^{15}N-labeled $(Ca^{2+})_4$-calmodulin (holo) was carried out. The spectral changes throughout the Tb^{3+} titration occur in slow exchange, as can be seen from the appearance of pseudocontact shifted signals due to the binding of Tb^{3+} ions to calmodulin (see Fig. 1). Signals from nuclei in the vicinity of the bound Tb^{3+} ions will show large pseudocontact shifts and significant broadening. By monitoring such effects on the assigned signals it could be determined that the Tb^{3+} ions bind first to the N-domain binding sites I and II.

The binding of Tb^{3+} ions to the N-domain gives rise to three paramagnetic species, according to whether Tb^{3+} binds separately to sites I or II, or simultaneously to both these sites. For each amide NH group there will be up to four signals in an ^1H-^{15}N HSQC spectrum: the signal corresponding to the $(Ca^{2+})_4$ species, and three signals corresponding to Tb^{3+}(I)-Ca^{2+}(II)-Ca^{2+}(III)-Ca^{2+}(IV), Ca^{2+}(I)-Tb^{3+}(II)-Ca^{2+}-(III)-Ca^{2+}(IV) and Tb^{3+}(I)-Tb^{3+}(II)-Ca^{2+}(III)-Ca^{2+}(IV)-calmodulin. Such patterns are seen throughout the spectrum for many residues.

Fig. 1A–D shows a section of the ^1H-^{15}N HSQC NMR spectrum containing the NH signal of residue Asn137 (C-domain) for different Tb^{3+} additions to $(Ca^{2+})_4$-calmodulin, namely $[Tb^{3+}]$/[CaM] ratios of 0, 0.33, 0.66 and 1.0 respectively. The gradual appearance of the three pseudocontact shifted signals corresponding to the species with bound Tb^{3+} in the N-domain sites can be followed throughout the titration. From the first addition of Tb^{3+}, the three Tb^{3+}-bound species are already present as can be seen in the spectrum recorded at a $[Tb^{3+}]$/[CaM] ratio of 0.33 (Fig. 1B). The most upfield signal of the four corresponds to the $(Tb^{3+})_2$ species (see below), and the two signals in between the first and fourth signals correspond to the signals from the two $(Tb^{3+})_1$ species. The assignments of these signals to Tb^{3+}(I)-Ca^{2+}(II)-Ca^{2+}(III)-Ca^{2+}(IV) and Ca^{2+}(I)-Tb^{3+}(II)-Ca^{2+}(III)-Ca^{2+}(IV)-calmodulin were made on the basis of the observed pseudocontact shift values. The signal from one of the two $(Tb^{3+})_1$ species is more intense than the other, reflecting a Tb^{3+} binding preference for site I rather than site II. The origin of this preference can be attributed to the higher negative charge of site I: there are four negatively charged side-chain ligands in site I (Asp20, Asp22, Asp24 and Glu31)

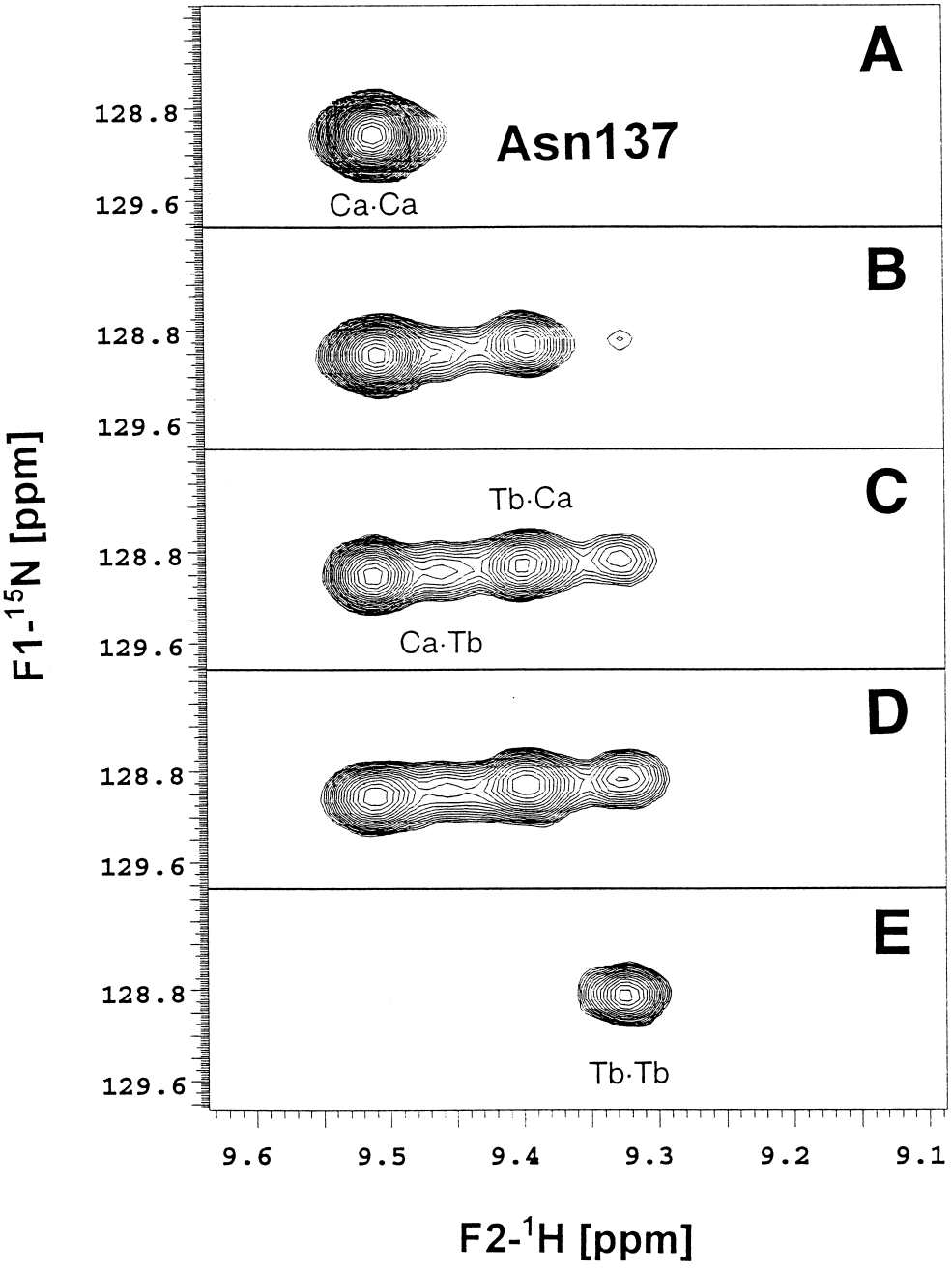

Fig. 1. A–D: Tb^{3+} titration of $(Ca^{2+})_4$-calmodulin monitored using ^1H-^{15}N HSQC spectra. The region of the spectra selected shows the NH signal of Asn 137 at $[Tb^{3+}]/[CaM]$ ratios of 0, 0.33, 0.66 and 1.0 in A, B, C and D respectively. The four signals shown in B, C and D correspond to, going in the upfield direction, the species $(Ca^{2+})_4$, Ca^{2+}(I)-Tb^{3+}(II)-Ca^{2+}(III)-Ca^{2+}(IV), Tb^{3+}(I)-Ca^{2+}(II)-Ca^{2+}(III)-Ca^{2+}(IV) and Tb^{3+}(I)-Tb^{3+}(II)-Ca^{2+}(III)-Ca^{2+}(IV)-calmodulin. E: Ca^{2+} titration of Tb^{3+}(I)-Tb^{3+}(II)-calmodulin monitored using ^1H-^{15}N HSQC spectra. The selected region of the spectrum is the same as in A and B and shows the NH signal of Asn137 at a $[Ca^{2+}]/[CaM]$ ratio of 0.66. The assignments of the different species are indicated on the spectra.

compared with only three in site II (Asp56, Asp58 and Glu67).

3.2. Tb^{3+}/Ca^{2+} titration of apo-calmodulin

Apo-calmodulin was titrated with $TbCl_3$ up to a $[Tb^{3+}]/[CaM]$ ratio of 2 and then with $CaCl_2$ up to a $[Ca^{2+}]/[CaM]$ ratio of 2. The changes throughout the titration were monitored using 2D ^1H-^{15}N HSQC NMR spectra.

The spectral changes observed in the Tb^{3+} titration occur in slow exchange and the binding of Tb^{3+} ions to apo-calmodulin gives rise to only one paramagnetic species, as can be seen from the appearance of one pseudocontact shifted signal. By monitoring the magnitude of the pseudocontact shifts and the broadening effects on the assigned signals it could be determined that the Tb^{3+} ions bind initially to the N-domain binding sites. The presence of only one paramagnetic signal throughout the Tb^{3+} titration indicates that Tb^{3+} fills simultaneously both sites I and II, therefore only the paramagnetic species Tb^{3+}(I)-Tb^{3+}(II)-calmodulin is obtained.

After the addition of $TbCl_3$, the sample was titrated with

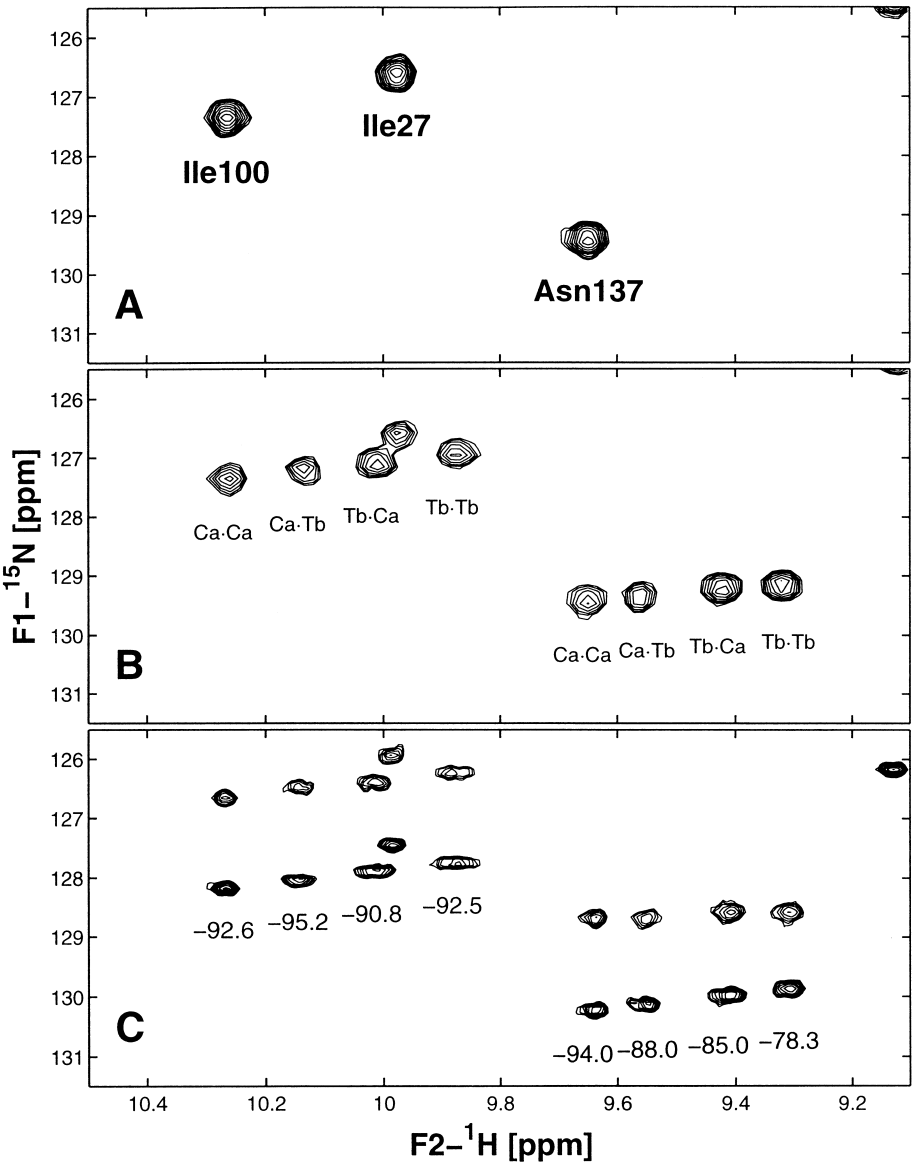

Fig. 2. A: A region of the ^{1}H-^{15}N HSQC spectrum for $(Ca^{2+})_4$-calmodulin-WFF showing the NH signals for Ile27, Ile100 and Asn137. B: The same region of the ^{1}H-^{15}N HSQC spectrum as in A for $(Ca^{2+})_4$-calmodulin-WFF with Tb^{3+} added to the sample at a $[Tb^{3+}]/[CaM]$ ratio of 0.66 showing the NH signals for Ile27, Ile100 and Asn137. The four signals for Ile100 and Asn137 correspond to, going in the upfield direction, the species $(Ca^{2+})_4$, Ca^{2+}(I)-Tb^{3+}(II)-Ca^{2+}(III)-Ca^{2+}(IV), Tb^{3+}(I)-Ca^{2+}(II)-Ca^{2+}(III)-Ca^{2+}(IV) and Tb^{3+}(I)-Tb^{3+}(II)-Ca^{2+}(III)-Ca^{2+}(IV)-calmodulin (the assignments are indicated on the spectrum). C: The same region of the ^{1}H-^{15}N IPAP-HSQC spectrum as in A and B for $(Ca^{2+})_4$-calmodulin-WFF with Tb^{3+} added to the sample at a $[Tb^{3+}]/[CaM]$ ratio of 0.66 showing both doublet components for the signals corresponding to the $(Ca^{2+})_4$ and Tb^{3+}/Ca^{2+} species found in B for Ile27, Ile100 and Asn137. The values for the one-bond ^{1}H-^{15}N splittings shown in the figure are in Hz.

$CaCl_2$. The spectral changes throughout the Ca^{2+} titration of Tb^{3+}(I)-Tb^{3+}(II)-calmodulin occur in slow exchange and the Ca^{2+} binds cooperatively to the C-domain binding sites III and IV as was observed previously for apo-calmodulin [9]. Signals from nuclei in C-domain residues, in both the apo and holo forms, are shifted due to the pseudocontact shifts from the two bound Tb^{3+} ions in the N-domain. This is demonstrated in the spectrum shown in Fig. 1E obtained following the addition of $CaCl_2$ to Tb^{3+}(I)-Tb^{3+}(II)-calmodulin at a $[Ca^{2+}]/[CaM]$ ratio of 0.66. Fig. 1E displays the same region of the ^{1}H-^{15}N HSQC spectrum as that in Fig. 1A–D, showing the signal corresponding to the backbone amide NH group of Asn137. This experiment allows the assignment of the Asn137 signal from the paramagnetic Tb^{3+}(I)-Tb^{3+}(II)-Ca^{2+}(III)-Ca^{2+}-(IV)-calmodulin species. For the Tb^{3+}(I)-Tb^{3+}(II) calmodulin species without bound Ca^{2+}, the Asn137 signal resonates in a different region of the spectrum. Similar behaviour can be observed for all other residues.

3.3. *PCS and RDC values in Ca^{2+}/Tb^{3+}-calmodulin-WFF and Ca^{2+}/Tb^{3+}-calmodulin*

In order to investigate the variation of the PCS and RDC values with differences in domain behaviour, these parameters were measured for the Ca^{2+}/Tb^{3+}-calmodulin-WFF and the Ca^{2+}/Tb^{3+}-calmodulin complexes. The Ca^{2+} ions bound to the N-domain of calmodulin in each system were partially

replaced by Tb^{3+} ion at a [Tb^{3+}]/[CaM] ratio of 0.66. At this concentration, the signals of the four species in solution show similar intensities and allow the convenient measurement of the differences in the ^1H-^{15}N splittings and chemical shifts for the four species simultaneously.

The binding of Tb^{3+} to both $(Ca^{2+})_4$-calmodulin systems follows the same order of binding with respect to the N- and C-domain metal binding sites. For each system examined at a [Tb^{3+}]/[CaM] ratio of 0.66, there are four predominant species in solution: diamagnetic $(Ca^{2+})_4$-calmodulin, and paramagnetic Tb^{3+}(I)-Ca^{2+}(II)-Ca^{2+}(III)-Ca^{2+}(IV), Ca^{2+}(I)-Tb^{3+}(II)-Ca^{2+}(III)-Ca^{2+}(IV) and Tb^{3+}(I)-Tb^{3+}(II)-Ca^{2+}(III)-Ca^{2+}(IV)-calmodulin. For each amide NH group there will be up to four signals corresponding to these species, three of which result from the pseudocontact shifts due to the presence of the paramagnetic Tb^{3+} ions bound to the N-domain of calmodulin. Fig. 2A,B shows a section of the ^1H-^{15}N HSQC spectrum for the calmodulin-WFF complex before and after the addition of Tb^{3+} at a [Tb^{3+}]/[CaM] ratio of 0.66. Fig. 2A shows the NH signals for residues Ile27, Ile100 and Asn137 of the diamagnetic $(Ca^{2+})_4$ species. Fig. 2B shows the additional signals of Ile100 and Asn137 for the paramagnetic Tb^{3+} species. The corresponding signals for the N-domain residue Ile27 cannot be seen in this section of the spectrum since they are greatly shifted and broadened by the nearby Tb^{3+} ions.

Pseudocontact shifts for NH protons and one-bond ^1H-^{15}N residual dipolar couplings were measured for both the Ca^{2+}/Tb^{3+}-calmodulin-WFF and the Ca^{2+}/ Tb^{3+}-calmodulin complexes, and Table 1 presents data measured for selected residues in both these systems to provide examples of the range of values obtained. The residues included in Table 1 were chosen from both domains, and show examples of both positive and negative pseudocontact shifts, and positive and negative dipolar coupling contributions to the NH splittings. For each residue shown in Table 1, the data measured for the four species in solution are given, except for the N-domain residues such as Gly33 or Ala57 for which the signals corresponding to some species could not be found. Both calmodulin systems show different PCSs and different RDCs for the same residues in the different systems, indicating differences in domain orientation and orientational freedom in both these systems. Table 1 also includes the distances from the backbone N atoms to the binding sites I and II measured for each residue from the available solution structure of the Ca^{2+}-bound calmodulin-MLCK peptide complex (2BBM in the Brookhaven PDB) [19]. These distances show that the Tb^{3+} ions perturb the chemical shifts of magnetic nuclei at distances extending over 40 Å.

The signals corresponding to the $(Ca^{2+})_4$ species are split only due to scalar coupling, $^1J_{NH}$ (ca. −94 Hz). Deviations from these splittings can be observed for the paramagnetic species for both systems, indicating alignment of the species containing Tb^{3+} ion induced by the external magnetic field. For the calmodulin-WFF complexes, Fig. 2C shows the one-

Table 1
Pseudocontact shifts and residual dipolar couplings for selected NH groups in Ca^{2+}/Tb^{3+}-calmodulin-WFF and Ca^{2+}/Tb^{3+}-calmodulin complexes

Residue	Ca^{2+}/Tb^{3+}-calmodulin-WFF						Ca^{2+}/Tb^{3+}-calmodulin			
	$r^a_{N(i)-Ca(I)}$	$r^b_{N(i)-Ca(II)}$	δ^H(NH)[c]	^{1}H PCS[d]	T^e_{NH}	D^f_{NH}	δ^H(NH)[c]	^{1}H PCS[d]	T^e_{NH}	D^f_{NH}
Gly33	9.80	16.42	8.74	**0.00**	−95.2	**0.0**	8.66	**0.00**	−94.8	**0.0**
			5.57	**−3.17**	−100.8	**−5.6**	n/a[g]	–	n/a	–
Gly40	18.08	24.44	7.83	**0.00**	−93.4	**0.0**	7.89	**0.00**	−95.1	**0.0**
			7.71	**−0.12**	−107.6	**−14.2**	7.80	**−0.09**	−94.6	**+0.5**
			7.13	**−0.70**	−96.0	**−2.6**	n/a	–	n/a	–
			7.00	**−0.83**	−110.7	**−17.3**	n/a	–	n/a	–
Ala57	16.62	5.12	8.03	**0.00**	−93.5	**0.0**	8.58	**0.00**	−94.2	**0.0**
			6.56	**−1.47**	−88.7	**+4.8**	7.34	**−1.24**	−89.4	**+4.8**
Ile100	30.37	36.31	10.27	**0.00**	−92.6	**0.0**	10.26	**0.00**	−92.7	**0.00**
			10.15	**−0.12**	−95.2	**−2.6**	10.23	**−0.03**	−92.5	**+0.2**
			10.02	**−0.25**	−90.8	**+1.8**	10.17	**−0.09**	−92.6	**+0.1**
			9.88	**−0.39**	−92.5	**−0.1**	10.11	**−0.15**	−92.5	**+0.2**
Leu116	22.31	33.06	8.11	**0.00**	−93.3	**0.0**	7.98	**0.00**	−93.5	**0.0**
			8.18	**+0.07**	−92.8	**+0.5**	8.01	**+0.03**	−93.4	**+0.1**
			8.32	**+0.21**	−86.8	**+6.5**	8.04	**+0.06**	−93.4	**+0.1**
			8.38	**+0.27**	−85.3	**+8.0**	8.06	**+0.08**	−94.3	**−0.8**
Asn137	32.70	37.34	9.64	**0.00**	−94.0	**0.0**	9.66	**0.00**	−93.8	**0.0**
			9.55	**−0.09**	−88.0	**+6.0**	9.61	**−0.05**	−93.4	**+0.4**
			9.41	**−0.23**	−85.0	**+9.0**	9.56	**−0.10**	−93.5	**+0.3**
			9.31	**−0.33**	−78.3	**+15.7**	9.50	**−0.16**	−92.8	+1.0

[a] Distance in Å from backbone N atom of residue *i* to Ca^{2+} in site I measured from the solution structure 2BBM (Brookhaven PDB) [19].
[b] Distance in Å from backbone N atom of residue *i* to Ca^{2+} in site II measured from the solution structure 2BBM (Brookhaven PDB) [19].
[c] ^{1}H chemical shift for NH groups in ppm referenced to DSS. For each residue, the value in the first row corresponds to the signal from the diamagnetic species, and the values in the following row/rows correspond to signals from the paramagnetic species.
[d] ^{1}H pseudocontact shifts values for NH groups obtained as the difference between the ^{1}H chemical shift for the signal being measured minus the ^{1}H chemical shift of the corresponding signal for the same residue in the diamagnetic $(Ca^{2+})_4$ species.
[e] ^{1}H-^{15}N splittings (T_{HN}), composed of scalar couplings ($^1J_{HN} \approx$ -94 Hz) and residual ^{1}H-^{15}N dipolar couplings (D_{HN}) (see [40]). These values are given in Hz with a minimum uncertainty of ±0.5 Hz and measured at 600 MHz. For each residue, the value in the first row corresponds to the splitting for the $(Ca^{2+})_4$ species, and the values in the following row/rows correspond to the splittings for the Tb^{3+}-bound species.
[f] Residual dipolar coupling (D_{NH}) contributions to one-bond ^{1}H-^{15}N splittings (T_{NH}) given in Hz and obtained as the difference between the one-bond ^{1}H-^{15}N splitting (T_{NH}) for the signal being measured minus the corresponding one-bond ^{1}H-^{15}N splitting ($^1J_{NH}$) for the same residue in the $(Ca^{2+})_4$ species ($D_{NH} = T_{NH}$-$^1J_{NH}$ as defined in reference [40]).
[g] Not assigned.

bond ^{1}H-^{15}N splittings from the IPAP HSQC spectrum corresponding to the same spectral region as that used in Fig. 2A,B. The splittings of the four signals for the NH group of Ile100 and Asn137 are indicated in Fig. 2C. For Ile100, the dipolar coupling contributions to the one-bond ^{1}H-^{15}N splittings are −2.6, +1.8 and −0.1 Hz for the three paramagnetic signals going in upfield direction. For Asn137, the dipolar coupling contributions to the one-bond ^{1}H-^{15}N splittings are +6.0, +9.0 and +15.7 Hz for the three paramagnetic signals going in upfield direction. The differences in dipolar coupling contributions to the splittings in the three paramagnetic species for the same NH group reflect the different relative orientations of the bond vectors with respect to the direction of the magnetic alignment tensor in each of these species.

4. Discussion

4.1. Choice of lanthanide

The ionic sizes and binding characteristics of trivalent lanthanide ions are similar to those of the Ca^{2+} ion [23] and lanthanide ions have frequently been used as paramagnetic probes for the Ca^{2+} ion in NMR studies [5,6]. For the applications discussed in the present work, an ideal lanthanide ion should bind selectively to its target molecule, should give rise to substantial RDC values from alignment of the molecule in a magnetic field, and should produce large PCS values for nuclei distant from the bound metal ion.

The degree of alignment of a paramagnetic species in an external magnetic field will depend on the degree of anisotropy of the magnetic susceptibility tensors [24]. Horrocks and Sipe have compared these for the entire lanthanide series of 4-picoline adducts, $Ln(dpm)_3(4\text{-pic})_2$ [25]. Their measured values show that Dy^{3+} ($4f^9$) and Tb^{3+} ($4f^8$) are the lanthanide ions with the highest magnetic susceptibility anisotropies.

Pseudocontact shifts also arise from the anisotropy of the magnetic susceptibility tensor of the lanthanide ion bound to the ligand molecule [26]. According to studies of Bleaney and coworkers, Tb^{3+} and Dy^{3+} are the lanthanide ions predicted to induce the largest pseudocontact shifts with Dy^{3+} showing the larger effects [27].

Thus, the high degree of magnetic susceptibility anisotropy of Tb^{3+} and Dy^{3+} makes these ions particularly powerful for obtaining information about nuclei at long distances from the Ln^{3+} ion due to their high RDC- and PCS-inducing abilities. However, the relaxation enhancement abilities of these ions are high as compared to the other lanthanides. Tb^{3+} was selected for this study because its broadening effect is only half that of Dy^{3+} [28]. The results reported here show that Tb^{3+} bound selectively to the N-domain of calmodulin can induce pseudocontact shifts for signals from nuclei at least in the range from 16 Å to more than 40 Å from the metal ion, and can produce magnetic alignments leading to substantial residual dipolar couplings.

4.2. Terbium binding to $(Ca^{2+})_4$-calmodulin systems

Tb^{3+} binds preferentially to the N-domain of $(Ca^{2+})_4$-calmodulin systems allowing different degrees of partial replacement by Tb^{3+} at the N-domain sites for different concentrations of added Tb^{3+}. Previous luminescence studies had also indicated that Tb^{3+} binds with a higher affinity to the N-domain than to the C-domain [29]. This behaviour contrasts with the binding of Ca^{2+} ions to calmodulin, which bind with higher affinity to the C-domain (sites III and IV), than to the N-domain sites (I and II) ([9] and references therein). These characteristics allow the selective replacement of Ca^{2+} with Tb^{3+} by carrying out Tb^{3+} titrations of $(Ca^{2+})_4$-calmodulin systems.

The NMR changes observed throughout the replacement of Ca^{2+} ions by Tb^{3+} occur in slow exchange at 14.1 T (^{1}H frequency of 600 MHz) yielding separate signals for species with bound Tb^{3+} ion/ions. The pseudocontact shifted signals that arise due to the Tb^{3+} binding to the N-domain can be assigned to the paramagnetic species Tb^{3+}(I)-Ca^{2+}(II)-Ca^{2+}-(III)-Ca^{2+}(IV), Ca^{2+}(I)-Tb^{3+}(II)-Ca^{2+}(III)-Ca^{2+}(IV) and Tb^{3+}-(I)-Tb^{3+}(II)-Ca^{2+}(III)-Ca^{2+}(IV)-calmodulin. For a nucleus sensing two paramagnetic metal ions, the total pseudocontact shift will be given by the sum of the two one-metal pseudocontact shifts [30]. The measured pseudocontact chemical shifts for each NH group in the $(Tb^{3+})_2$ species examined here are essentially equal to the sum of the values observed for the two $(Tb^{3+})_1$ species: this additivity of shifts from different species is an indication that the replacement of Ca^{2+} by Tb^{3+} is not accompanied by large overall structural changes.

The degree of protein alignment obtained by partial replacement of Ca^{2+} by Tb^{3+} in calmodulin systems is sufficiently large to produce substantial dipolar coupling contributions to the one-bond ^{1}H-^{15}N splittings (and the same will probably be true for ^{1}H-^{13}C splittings). The values of the residual dipolar couplings measured from the one-bond ^{15}N-^{1}H splittings are up to 17 Hz in magnitude, and these values are quite large compared with residual dipolar couplings measured in other magnetically aligned paramagnetic biomolecules [2,31].

The differently shifted signals from the corresponding NH group in the different species allow the independent measurement of ^{1}H-^{15}N residual dipolar couplings for the different Tb^{3+}-bound species in the same sample. The NH signals from the diamagnetic $(Ca^{2+})_4$-calmodulin provide internal standards for the isotropic splittings (assuming no significant magnetic alignment of the diamagnetic species). The different Tb^{3+}-bound species will provide different alignments and these can be useful as a means of resolving orientational degeneracy in dipolar coupling-based structural calculations [32].

The binding of Tb^{3+} to apo-calmodulin shows intradomain cooperativity (as seen for Ca^{2+} ([33] and references therein). The fact that the Tb^{3+} titration of apo-calmodulin gives rise to only one paramagnetic species in solution with Tb^{3+} ions bound simultaneously to the N-domain sites I and II (no species with one metal ion bound was detected) is consistent with positive intradomain Tb^{3+}/Tb^{3+} cooperativity of metal binding. The titration data of $(Ca^{2+})_4$-calmodulin with Tb^{3+} are consistent with intradomain Tb^{3+}/Ca^{2+} binding cooperativity in each $(Tb^{3+})_1$ species. Evidence for intradomain Ce^{3+}/Ce^{3+} binding cooperativity in calmodulin has been reported by Bentrop and coworkers [6]. The intradomain cooperativity between metal ions (Ca/Ca, Tb/Ca, Tb/Tb, Ce/Ce) in EF-hand pairs can be ascribed at least partly to short-range cooperative cyclic interactions [34].

4.3. Conformational behaviour of calmodulin domains in solution

The $(Ca^{2+})_4$-calmodulin-WFF complex adopts a single conformation for the two domains [19] as is the case for other

structures of $(Ca^{2+})_4$-calmodulin complexed with peptides from target enzymes [35]. The WFF peptide, encompassing the calmodulin-binding region of skMLCK, adopts a helical conformation and binds to both domains of calmodulin. The structure of the complex is stabilised mainly by the interaction of two key 'hydrophobic anchor' residues in the peptide, namely Trp4 and Phe17, with the C- and N-domains respectively. These interactions result in the fixing of the domains [19]. Such systems exist in a single conformation, and hence measurements of their RDC and PCS values using partial replacement of Ca^{2+} by Tb^{3+} should allow the determination of the relative orientation of the domains.

For $(Ca^{2+})_4$-calmodulin in solution, both domains are essentially free from each other and connected by a highly flexible linker [7]. The structure of each domain in solution has been determined using NOE-based methods [1]. Since in this system the two domains are not held in a single fixed conformation, the measured RDC and PCS values provide only a qualitative guide to the average disposition of the two domains.

A consideration of the parameters measured for the Ca^{2+}/Tb^{3+}-calmodulin complexes with those for the Ca^{2+}/Tb^{3+}-calmodulin-WFF complexes allows a qualitative comparison.

(i) Ca^{2+}/Tb^{3+}-calmodulin complexes show smaller PCS values than the Ca^{2+}/Tb^{3+}-calmodulin-WFF complexes, suggesting that the domains in the former system are further apart on average. These results are in good agreement with recent small-angle X-ray scattering measurements that showed that the radius of gyration (R_g) and the maximum dimension (d_{max}) for $(Ca^{2+})_4$-calmodulin are larger than for the $(Ca^{2+})_4$-calmodulin-peptide complex (R_g of 20.3 ± 0.7 Å and 16.4 ± 0.2 Å respectively, and d_{max} of 61 Å and 49 Å respectively) ([36] and references therein).

(ii) The C-domain backbone NH groups of the Ca^{2+}/Tb^{3+}-calmodulin system also show smaller RDC values than those of Ca^{2+}/Tb^{3+}-calmodulin-WFF system indicating that the degree of alignments in the former are smaller than in the latter. The smaller C-domain RDC values reflect a higher degree of orientational freedom between the domains in the Ca^{2+}/Tb^{3+}-calmodulin system. For systems where the calmodulin domains have fixed orientations with respect to one another, the transmission of alignment from the paramagnetic N-domain to the diamagnetic C-domain will be 100% and the RDC values of both the C- and N-domains will depend on the relative orientations of the bond vectors to the molecular alignment tensor.

5. Concluding remarks

The classical mode of interaction of calmodulin with target peptide sequences has been well described by NMR and X-ray methods (reviewed by Crivici and Ikura [35]). Recent work indicates the potential diversity of binding modes of calmodulin for its targets which emphasise the need for general methods of determining domain orientations in complexes of calmodulin with target proteins [37–39].

The results presented in this work show that calmodulin complexes containing Tb^{3+} ions bound to only one of its domains allow the measurement of interdomain pseudocontact shifts and significant residual dipolar couplings, and that these can be used for monitoring long-range interdomain phenomena. The fact that addition of the PCS values of the $(Tb^{3+})_1$ species yields the PCS values of the $(Tb^{3+})_2$ species indicates that the replacement of Ca^{2+} by Tb^{3+} ions does not affect the overall structure.

The simultaneous determination of long-range pseudocontact shifts and residual dipolar couplings can provide a powerful NMR approach for determining the relative orientations of the domains in Ca^{2+}-binding proteins that have fixed domain orientations. Such systems will be found in many complexes of Ca^{2+}-binding proteins with their target proteins and peptides. Similar complexes with mutant or chimera proteins could also be studied in this way.

Acknowledgements: We are grateful to Kathy Beckingham for supplying the pOTSNco12 vector containing the cDNA coding for *Drosophila melanogaster* calmodulin, to John E. McCormick for expert technical assistance, to Tom A. Frenkiel for assistance with the NMR experiments, and to Geoffrey Kelly and Annalisa Pastore for useful discussions and critical reading of the manuscript.

References

[1] Ikura, M., Spera, S., Barbato, G., Kay, L.E., Krinks, M. and Bax, A. (1991) Biochemistry 30, 9216–9228.
[2] Tolman, J.R., Flanagan, J.M., Kennedy, M.A. and Prestegard, J.H. (1995) Proc. Natl. Acad. Sci. USA 92, 9279–9283.
[3] Bax, A. and Tjandra, N. (1997) J. Biomol. NMR 10, 289–292.
[4] Fischer, M.W.F., Losonczi, J.A., Weaver, J.L. and Prestegard, J.H. (1999) Biochemistry 38, 9013–9022.
[5] Lee, L. and Sykes, B.D. (1983) Biochemistry 22, 4366–4373.
[6] Bentrop, D., Bertini, I., Cremonini, M.A., Forsén, L., Luchinat, C. and Malmendal, A. (1997) Biochemistry 36, 11605–11618.
[7] Barbato, G., Ikura, M., Kay, L.E., Pastor, R.W. and Bax, A. (1992) Biochemistry 31, 5269–5278.
[8] Kretsinger, R.H. and Nockolds, C.E. (1973) J. Biol. Chem. 248, 3313–3326.
[9] Biekofsky, R.R., Martin, S.R., Browne, J.P., Bayley, P.M. and Feeney, J. (1998) Biochemistry 37, 7617–7629.
[10] Maune, J.F., Klee, C.B. and Beckingham, K. (1992) J. Biol. Chem. 267, 5286–5295.
[11] Ikura, M., Kay, L.E., Krinks, M. and Bax, A. (1990) Biochemistry 29, 4659–4667.
[12] Gill, S.C. and von Hippel, P.H. (1989) Anal. Biochem. 182, 319–326.
[13] States, D.J., Haberkorn, X. and Ruben, D.J. (1982) J. Magn. Reson. 48, 286–292.
[14] Bodenhausen, G. and Ruben, D.J. (1980) Chem. Phys. Lett. 69, 185–191.
[15] Mori, S., Abeygunawardana, C., O'Neil Johnson, M. and van Zijl, P.C.M. (1995) J. Magn. Reson. B 108, 94–98.
[16] Ottiger, M., Delaglio, F. and Bax, A. (1998) J. Magn. Reson. 131, 373–378.
[17] Bartels, C., Xia, T., Billeter, M., Güntert, P. and Wüthrich, K. (1995) J. Biomol. NMR 5, 1–10.
[18] Schmidt, J.M., Ernst, R.R., Saburo, A. and Kainosho, M. (1995) J. Biomol. NMR 6, 95–105.
[19] Ikura, M., Clore, G.M., Gronenborn, A.M., Zhu, G., Klee, C.B. and Bax, A. (1992) Science 256, 632–638.
[20] Wishart, D.S., Bigam, C.G., Yao, J., Abildgaard, F., Dyson, H.J., Oldfield, E., Markley, J.L. and Sykes, B.D. (1995) J. Biomol. NMR 6, 135–140.
[21] Zhang, M., Tanaka, T. and Ikura, M. (1995) Nature Struct. Biol. 2, 758–767.
[22] Ikura, M., Kay, L.E., Krinks, M. and Bax, A. (1991) Biochemistry 30, 5498–5504.
[23] Snyder, E.E., Buoscio, B.W. and Falke, J.J. (1990) Biochemistry 29, 3937–3943.
[24] Bothner-By, A.A. (1996) Encyclopedia in Nuclear Magnetic Resonance (Grant, D.M. and Harris, R.K., Eds.), pp. 2932–2938, Wiley, Chichester.
[25] Horrocks Jr., W.D. and Sipe III, J.P. (1972) Science 177, 994.
[26] Inagaki, F. and Miyazawa, T. (1981) Prog. NMR Spectrosc. 14, 67–111.

[27] Bleaney, B., Dobson, C.M., Levine, B.A., Martin, R.B., Williams, R.J.P. and Xavier, A.V. (1972) J. Chem. Soc. Chem. Commun., 791–793.
[28] Horrocks Jr., W.D. and Sipe III, J.P. (1971) J. Am. Chem. Soc. 93, 6800.
[29] Wang, C.-L.A., Leavis, P.C. and Gergely, J. (1984) Biochemistry 23, 6410–6415.
[30] Bertini, I. and Luchinat, C. (1996) Coord. Chem. Rev. 150, 131–161.
[31] Banci, L., Bertini, I., Huber, J.G., Luchinat, C. and Rosato, A. (1998) J. Am. Chem. Soc. 120, 12903–12909.
[32] Ramirez, B.E. and Bax, A. (1998) J. Am. Chem. Soc. 120, 9106–9107.
[33] Linse, S. and Chazin, W.J. (1995) Protein Sci. 4, 1038–1044.
[34] Biekofsky, R.R. and Feeney, J. (1998) FEBS Lett. 439, 101–106.
[35] Crivici, A. (1995) Annu. Rev. Biophys. Biomol. Struct. 24, 85–116.
[36] Osawa, M., Kuwamoto, S., Izumi, Y., Yap, K.L., Ikura, M., Shibanuma, T., Yokokura, H., Hidaka, H. and Matsushima, N. (1999) FEBS Lett. 442, 173–177.
[37] Bayley, P.M., Findlay, W.A. and Martin, S.R. (1996) Protein Sci. 5, 1215–1228.
[38] Barth, A., Martin, S.R. and Bayley, P.M. (1998) J. Biol. Chem 273, 2174–2183.
[39] Rhoads, A.R. and Friedberg, F. (1997) FASEB J. 11, 331–340.
[40] Annila, A., Aitio, H., Thulin, E. and Drakenberg, T. (1999) J. Biomol. NMR 14, 223–230.